

Stacking Transformation from Hexagonal to Cubic SiC Induced by Surface Reconstruction: A Seed for Heterostructure Growth

U. Starke,* J. Schardt, J. Bernhardt, M. Franke, and K. Heinz

Lehrstuhl für Festkörperphysik, Universität Erlangen-Nürnberg, Staudstrasse 7, D-91058 Erlangen, Germany

(Received 5 October 1998)

Promoted by Si enrichment during the formation of the reconstructed $(\sqrt{3} \times \sqrt{3})R30^\circ$ phase on hexagonal SiC(0001) a cubic stacking sequence develops at the surface. The reconstruction is ultimately resolved to consist of Si adatoms in T_4 sites as found by quantitative LEED crystallography. Prior to the $(\sqrt{3} \times \sqrt{3})R30^\circ$ phase evolution mesalike structures with various atomic periodicities are observed by STM. Smoothing of this rough and Si enriched state provides the material for the formation of the modified stacking sequence which could serve as seed for preparation of SiC polytype heterostructures. [S0031-9007(99)08644-5]

PACS numbers: 68.35.Bs, 61.14.Hg, 61.16.Ch, 61.72.Nn

Technological application in high power and high temperature devices has made silicon carbide an important semiconductor material. One of its most puzzling physical properties is the occurrence of polytypes distinguished by the stacking of adjacent SiC bilayers. As their total energies are very similar, i.e., different by only a few meV per SiC pair [1], the controlled growth of single polytype material without grain boundaries is difficult. Also, heterostructures of different polytypes prospectively useful due to their different band gaps have not yet been successfully grown despite their ideal lattice matching.

The stacking sequence of a given polytype can be copied by attaching new material at step edges of a substrate cut slightly tilted with respect to the basal plane (*off axis*), thus establishing a step flow growth mode [2]. It has been shown for SiC(0001) that its (3×3) surface reconstruction minimizes the number of dangling bonds [3] which enhances the necessary diffusion of incoming particles. Yet, for the formation of heterostructures the layer stacking needs to be changed rather than copied from the substrate, and so a flat rather than stepped surface should be used. Then, however, island nucleation is observed leading to a large number of grain boundaries which spoils the formation of a sharp heterostructure junction. Recent reports of a layer-by-layer growth of SiC films by periodically generating different superstructures, namely, the (3×3) , $(\sqrt{3} \times \sqrt{3})R30^\circ$, and a disordered (1×1) phase [4] suggest that the surface reconstruction might influence the stacking of newly attached bilayers. Yet, the physics behind and, in particular, the atomic geometry of the phases involved remain unclear.

In the present paper we provide new and precise structural information about the $(\sqrt{3} \times \sqrt{3})R30^\circ$ superstructure and the underlying substrate by quantitative low-energy electron diffraction (LEED) structure analysis. With the unambiguous identification of Si adatoms in so-called T_4 positions [5], we resolve an old controversy. Even more important we demonstrate that during the formation of the $(\sqrt{3} \times \sqrt{3})R30^\circ$ superstructure a cubic stacking sequence can be induced despite the hexagonal

nature of the 4H-SiC substrate used. We give evidence that prolonged annealing in the presence of excess silicon is essential for the new stacking to develop. During the formation of the stacking rearrangement we observe a rather rough surface with a variety of different periodic structures appearing in mesalike domains while the fully ordered $(\sqrt{3} \times \sqrt{3})R30^\circ$ surface displays large flat terraces using scanning tunneling microscopy (STM). This suggests that—induced by the $(\sqrt{3} \times \sqrt{3})R30^\circ$ reconstruction pattern—the material available during the smoothing of the rough surface state is used for the continuation of a cubic stacking sequence at the surface.

The experiments were carried out in an ultrahigh vacuum (UHV) chamber allowing for routine sample introduction and transfer between stages for LEED, STM, and silicon evaporation. The reconstruction geometry of the $(\sqrt{3} \times \sqrt{3})R30^\circ$ superstructure and the stacking sequence of the first few SiC bilayers were determined by LEED structure analysis. Diffraction spot intensities, $I(E)$ spectra, were recorded from a 4-grid LEED optics using a video based data acquisition system [6]. Dynamical intensity calculations were carried out using, in particular, the tensor LEED algorithm [6,7]. The Pendry R factor R_p [8] was used to guide an automated search algorithm [9] in order to identify the best-fit structure including the relative weights of domains exhibiting different surface layer stacking as practiced successfully earlier [10,11]. STM images were acquired to provide additional information about the topmost layer of the reconstruction phase and—even more important—to determine morphology changes and local periodicities during the development of the $(\sqrt{3} \times \sqrt{3})R30^\circ$ phase.

A 4H-SiC film sample homoepitaxially grown by chemical vapor deposition (CVD) [12] was used. The sample was etched *ex situ* by annealing at 1550 °C under hydrogen gas flow using a CVD reactor. Inside the UHV chamber it immediately displayed a $(\sqrt{3} \times \sqrt{3})R30^\circ$ phase which, however, corresponds to a silicon oxide adlayer whose structure is discussed elsewhere [13]. Upon annealing around 1000 °C the oxide layer desorbs

and the $(\sqrt{3} \times \sqrt{3})R30^\circ$ phase discussed in the present context develops. In addition to this simple method of just heating the *ex situ* prepared sample [14], two other recipes were used involving the deposition of excess Si during annealing. Depending on the sample temperature and Si flux chosen, either the $(\sqrt{3} \times \sqrt{3})R30^\circ$ phase develops immediately [15] or starting from the silicon rich (3×3) phase [3] the $(\sqrt{3} \times \sqrt{3})R30^\circ$ phase is formed by annealing [16,17].

Quantitative LEED analyses carried out for each preparation method result in optimized model structures that are characterized by the same reconstruction pattern: a Si adatom in the T_4 position as displayed in Fig. 1a. R factors of $R_p = 0.11$ – 0.13 , which is extremely low and convincing for a structure of such complexity, were obtained for the three cases (see Table I for details). Other feasible models, in particular, those discussed in the literature, e.g., adatom in H_3 site (threefold coordinated hollow), Si trimer or tetramer clusters, and carbon rich structures could be ruled out in view of R factors larger than 0.6. Even a carbon adatom in the T_4 position, which geometrically is identical to our favorite model and differs only by the scattering properties of the adatom, yields a significantly worse fit ($R_p = 0.19$) together with an unphysical C–Si bond length. The clear R -factor distinction from alternative models [18] and the excellent level of agreement make the T_4 silicon adatom model unambiguous, so solving an old problem extensively discussed in the literature. This is of importance as the model had been favored by theoretical work using density functional theory (DFT) [19–21], yet was at variance with quantum chemical [22] and other experimental [15,23] studies. Additionally, DFT predicted the T_4 reconstructed surface to be metallic, while experimental work finds a surface gap [23,24]. Though this latter discrepancy could be resolved by the assumption of large electronic correlation effects [25] making the surface semiconducting, the situation remained uncertain with respect to the real surface structure. So, a crystallographic structure determination

as in the present work was timely, even explicitly demanded [25]. It settles the issue in favor of the T_4 adatom model.

In addition to solving the fundamental problem of the $(\sqrt{3} \times \sqrt{3})R30^\circ$ reconstruction geometry we found a rearrangement of the substrate stacking sequence. This latter result may be a key issue for the growth of polytype heterostructures. Unexpectedly, the overall best R factor of 0.11 for the structure prepared from the (3×3) phase could be achieved only by considering domains with a surface terminating bilayer stacking sequence incompatible with the $4H$ bulk structure. Ideally the bulk stacking sequence of $4H$ -SiC, $[ABCBA] \dots$, allows only two types of stacking terminations at the surface, either $ABCBA \dots$ ($S2$) or $BCBAB \dots$ ($S1$), cf. Fig. 1b [26]. However, regardless of the mixing ratio of the stacking domains the correspondence between experimental and calculated intensities was unsatisfying ($R_p \geq 0.26$). Only the inclusion of an *additional* domain type with a third bilayer in the same orientation on top ($S3$ stacking, $CABCBA \dots$; cf. Fig. 1b) could improve the fit with a drastic reduction of the R factor from 0.26 to 0.11. In the optimized structure a fraction of 65% of the surface consists of domains with this unusual stacking sequence, i.e., three identically oriented bilayers at the topmost surface which is incompatible with the $4H$ bulk stacking but the basic element of $3C$ - and $6H$ -SiC polytypes. The area of the surface covered with these domains strongly depends on the amount of silicon exposure during the preparation of the $(\sqrt{3} \times \sqrt{3})R30^\circ$ phase. When prepared directly by heating in a smaller Si flux, we find only 35% of the surface covered by $S3$ terminated areas; when prepared from an *ex situ* pretreated sample by heating alone, a negligible amount of the surface displays $S3$ stacking [27]. The respective domain weights are listed in Table I.

The main reconstruction parameters, i.e., adatom layer spacing d_{01} , silicon bond length L_{01} , and a surface buckling b_2 below the adatom (cf. Fig. 1a) compare very well for the differently prepared surfaces (variations are below our approximate error margin [18], i.e., ± 0.05 Å). This means that the adatom geometry is dominated by the local bonding rearrangement in the reconstruction and not affected by different stacking of deeper bilayers. The values are also in good agreement with DFT results [19,21] as shown in Table II. Other substrate geometry parameters

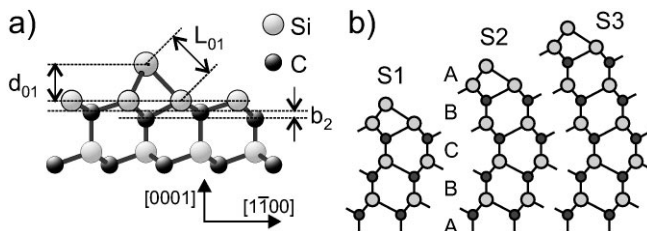


FIG. 1. T_4 model for the $(\sqrt{3} \times \sqrt{3})R30^\circ$ phase on SiC(0001) displayed in a side view projection along the $[11\bar{2}0]$ direction. (a) Si adatom fourfold coordinated to three Si and one C atom of the topmost substrate bilayer. Geometry parameters as given in Table II are indicated. (b) Different stacking terminations denoted $S1$, $S2$, or $S3$ according to the number of identically oriented bilayers at the surface in accordance to previous papers [10,11,17]. Note that the $S3$ termination is breaking the $4H$ bulk stacking sequence.

TABLE I. Weights of domains with different surface terminating stacking sequences and Pendry R factors derived for the optimized geometries of the three differently prepared $(\sqrt{3} \times \sqrt{3})R30^\circ$ structures.

Preparation method	Pendry R factor	Surface stacking		
		$S2$	$S1$	$S3$
Annealing <i>ex situ</i> sample	0.13	75%	15%	10%
Direct prep. in Si-flux	0.13	50%	15%	35%
Annealing (3×3) phase	0.11	20%	15%	65%

TABLE II. Structural parameters as defined in Fig. 1a determined for the $(\sqrt{3} \times \sqrt{3})R30^\circ$ superstructure by LEED (present work, error limits about ± 0.05 Å) and by DFT. LEED results are averaged over values obtained for the different domains of the best-fit structure.

Parameters	From LEED	From DFT	
	(this work)	Ref. [19]	Ref. [21]
d_{01} (Å)	1.77	1.75	1.71
b_2 (Å)	0.34	0.22	0.25
L_{01} (Å)	2.46	2.42	2.41

varied down to the sixth atomic layer were found to be practically bulklike except for a slight contraction by 0.05 Å of the topmost SiC bilayer and some buckling below the adatom in the second layer (0.12 Å).

The nature of the stacking rearrangement which is promoted when the $(\sqrt{3} \times \sqrt{3})R30^\circ$ structure is prepared by annealing the Si rich (3×3) phase was further illuminated by investigating the transition state between the (3×3) and the final phase. During annealing the starting structure at 1000 °C the surface passes through several intermediate phases as displayed in the LEED patterns of Fig. 2. A mixture of (3×3) and (2×2) structures (Fig. 2a) is followed by a streaky phase (Fig. 2b) until eventually the $(\sqrt{3} \times \sqrt{3})R30^\circ$ phase develops in practically perfect order (Fig. 2c). This transition is accompanied by a dramatic reordering of the surface as evident from STM. As demonstrated in Fig. 3a, large mesalike structures develop which display patches of different periodicity on top. The mesa shown in the figure contains different locally order areas of $(4\sqrt{7} \times 4\sqrt{7})R19.1^\circ$ and (4×4) periodicity as indicated in the enlargements. This rough morphology is not present in the initial (3×3) phase [17] and again disappears when the $(\sqrt{3} \times \sqrt{3})R30^\circ$ phase is fully ordered as shown in Fig. 3b.

The reproducible stacking rearrangement can be envisaged as seed for $3C$ or $6H$ polytype stacking and might provide a chance for a controlled preparation of heterostructures. Our findings might also improve the fundamental understanding of polytypism. Surface energies and geometries of the $(\sqrt{3} \times \sqrt{3})R30^\circ$ phase have been

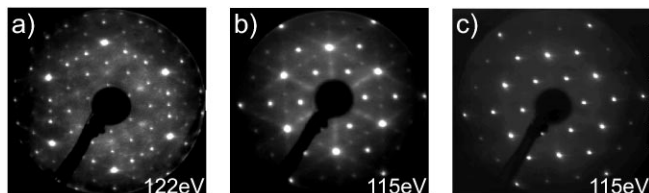


FIG. 2. LEED patterns (normal incidence) monitoring annealing of the (3×3) phase at 1000 °C. (a) Mixed phase of (3×3) and (2×2) periodicity after 10 min. (b) Incomplete $(\sqrt{3} \times \sqrt{3})R30^\circ$ phase with streaks between the integer order spots after 20 min. (c) Ordered $(\sqrt{3} \times \sqrt{3})R30^\circ$ phase after 30 min.

investigated on $3C$ and $2H$ polytypes [20]. In agreement with our results the reconstruction geometry was found to be fairly independent of the substrate stacking. The energy differences between the two polytypes were found to be rather small, so that the surface energy alone should not induce the modified stacking. Rutter and Heine [28] found a preference for a 60° rotation of the top bilayer, i.e., a hexagonal termination on a $3C$ -SiC surface again with only little energy decrease, yet without including superstructures in their calculations due to computational limitations. In earlier work by Heine *et al.* [29], also for unreconstructed surfaces, a new layer was predicted to be attached in cubic stacking during growth, yet without considering the entropy term in the energy calculations.

Pretty safely, we can rule out that the $S3$ stacking develops from a bilayer rotation on $S1$ domains, because before and after desorbing the oxide layer only 15% of the surface display $S1$ stacking (see Ref. [13] and Table I). It is rather the 75%–85% of $S2$ domains that appear to transform into $S3$ domains which suggests a new, identically oriented bilayer to be attached on top of the old domains. As apparent from the STM images, the preparation under Si rich conditions causes the surface to roughen intermediately. The disappearance of the mesas with the excess Si finally desorbing must be accompanied by a considerable material transport which enables the new bilayer to form. That it continues the orientation of the layers already present and thus forms a cubic stacking inconsistent with the $4H$ bulk structure is obviously caused by the excess silicon in view of the $S3$ termination being found only when the surface is Si enriched during the preparation. This is supported in addition by the fact that the area of $S3$ stacking is reduced again when the surface is further heated in reduced Si flux [the method that immediately results in the $(\sqrt{3} \times \sqrt{3})R30^\circ$ structure]. So, even if the cubic

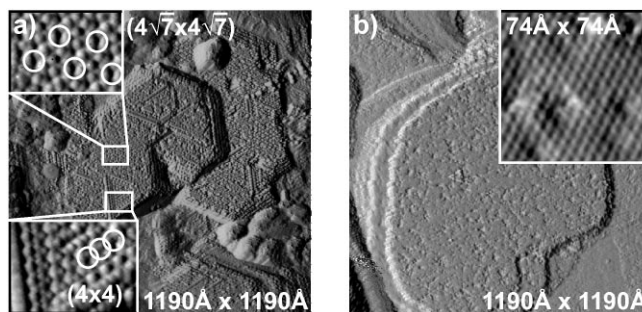


FIG. 3. (a) STM image of a ca. 600 Å wide mesa in the phase transformation region corresponding to the streaky LEED pattern (Fig. 2b). Selected patches with particular local periodicity are enlarged on the left side. The periodicity is indicated by the circles. ($U_{\text{tip}} = 1.42$ V, $I = 0.4$ nA.) (b) Flat, large terrace of the well ordered $(\sqrt{3} \times \sqrt{3})R30^\circ$ structure corresponding to the LEED pattern in Fig. 2c. Note that the inset showing atomic resolution is taken from a smaller scan. ($U_{\text{tip}} = -0.8$ V, $I = 0.2$ nA.)

stacking of the new layer may be slightly favored by the $(\sqrt{3} \times \sqrt{3})R30^\circ$ reconstruction geometry due to subtle energetic differences (which we cannot decide from the present results) it is certainly initiated by the silicon enrichment and the mesa disappearance. We recall that on an *ex situ* pretreated sample with only *S2* and *S1* domains [13] no appreciable stacking rearrangement is observed when the $(\sqrt{3} \times \sqrt{3})R30^\circ$ phase is formed by annealing alone. This indicates that the unusual surface layer stacking requires a kinetic effect that is more important than small energy differences.

In conclusion we have identified the reconstruction geometry of the $(\sqrt{3} \times \sqrt{3})R30^\circ$ phase on *4H-SiC*(0001) as a *T₄* site Si adatom model. The model parameters were precisely determined. This solves a long-standing issue and supports the theoretical proposal of electronic correlation effects to explain the semiconducting nature of this phase. More importantly we have detected a rearrangement of the surface stacking different from that of normal *4H-SiC* which is obviously kinetically triggered when the superstructure is prepared from a sufficiently Si enriched surface. The new stacking sequence resembles a part of the *3C* or *6H* polytype unit cell. This is of importance for semiconductor technology as it might provide a recipe to generate SiC heterostructures.

We thank A. Schöner and N. Nordell for providing SiC samples and K. Christiansen for helping with the hydrogen etching procedure. This work was supported by the Deutsche Forschungsgemeinschaft through SFB 292.

*Corresponding author: fax: +49-9131-85-28400

Email: ustarke@fkp.physik.uni-erlangen.de

- [1] C. Cheng, V. Heine, and R.J. Needs, *Europhys. Lett.* **12**, 69 (1990).
- [2] H.S. Kong, J.T. Glass, and R.F. Davis, *J. Appl. Phys.* **64**, 2672 (1988); T. Kimoto, A. Itoh, and H. Matsunami, *J. Appl. Phys.* **81**, 3494 (1997); A. Fissel, B. Schröter, and W. Richter, *Appl. Phys. Lett.* **66**, 3182 (1995).
- [3] U. Starke *et al.*, *Phys. Rev. Lett.* **80**, 758 (1998).
- [4] A. Fissel *et al.*, *Appl. Phys. Lett.* **68**, 1204 (1996).

- [5] Threefold hollow adatom position on Top of a second layer atom, thus effectively 4-fold coordinated.
- [6] K. Heinz, *Rep. Prog. Phys.* **58**, 637 (1995).
- [7] P.J. Rous, *Prog. Surf. Sci.* **39**, 3 (1992).
- [8] J.B. Pendry, *J. Phys. C* **13**, 937 (1980).
- [9] M. Kottcke and K. Heinz, *Surf. Sci.* **376**, 352 (1997).
- [10] U. Starke, *Phys. Status Solidi (b)* **202**, 475 (1997).
- [11] J. Schardt *et al.*, *Surf. Rev. Lett.* **5**, 181 (1998).
- [12] N. Nordell, A. Schöner, and S.G. Andersson, *J. Electrochem. Soc.* **143**, 2910 (1996).
- [13] J. Bernhardt *et al.*, *Appl. Phys. Lett.* (to be published).
- [14] F. Owman and P. Martensson, *Surf. Sci. Lett.* **330**, L639 (1995); U. Starke *et al.*, *Appl. Surf. Sci.* **89**, 175 (1995).
- [15] L. Li *et al.*, *J. Appl. Phys.* **80**, 2524 (1996).
- [16] R. Kaplan, *Surf. Sci.* **215**, 111 (1989).
- [17] U. Starke, J. Schardt, and M. Franke, *Appl. Phys. A* **65**, 578 (1997).
- [18] Models yielding $R_p \geq R_{p,opt} + RR$ can be significantly excluded based on statistical grounds, *RR* being the variance of the Pendry *R* factor [8]. For our best-fit model with $R_{p,opt} = 0.107$ this variance is $RR = 0.016$.
- [19] J.E. Northrup and J. Neugebauer, *Phys. Rev. B* **52**, R17001 (1995).
- [20] F. Bechstedt *et al.*, *Phys. Status Solidi (b)* **202**, 35 (1997).
- [21] J. Pollmann, P. Krüger, and M. Sabisch, *Phys. Status Solidi (b)* **202**, 421 (1997).
- [22] P. Badziag, *Surf. Sci.* **337**, 1 (1995).
- [23] L.I. Johansson, F. Owman, and P. Martensson, *Surf. Sci. Lett.* **360**, L478 (1996); **360**, L483 (1996).
- [24] J.-M. Themlin *et al.*, *Europhys. Lett.* **39**, 61 (1997).
- [25] J.E. Northrup and J. Neugebauer, *Phys. Rev. B* **57**, R4230 (1998).
- [26] Stacking sequences *CBABC...* and *BABCB...* are symmetry equivalent to *S1* and *S2* but rotated by 60°. As judged from the sixfold symmetric LEED pattern both orientations of each stacking type are present in equal amounts.
- [27] Based on the *R*-factor variance [18], the error bar for determining a domain percentage is approximately 15%. Thus, 10% as obtained for the *S3* termination in case of the *ex situ* pretreated sample is insignificant.
- [28] M.J. Rutter and V. Heine, *J. Phys. CM* **9**, 8213 (1997).
- [29] V. Heine, C. Cheng, and R.J. Needs, *J. Am. Ceram. Soc.* **74**, 2630 (1991).